Pergamon

Int. J. Heat Mass Transfer. Vol. 41, Nos 8–9, pp. 1103–1112, 1998

Printed in Great Britain
0017–9310/98 $19.00+0.00

PII: S0017–9310(97)00167–1

One-group interfacial area transport in vertical bubbly flow

Q. WU, S. KIM and M. ISHII
Thermal Hydraulics and Reactor Safety Laboratory, Purdue University, West Lafayette, IN 47907, U.S.A.

and

S. G. BEUS
Bettis Atomic Power Laboratory, Westinghouse Electric Corporation, Box 79, West Mifflin, PA 15122, U.S.A.

(*Received* 20 *February* 1997 *and in final form* 28 *May* 1997)

Abstract—In the two-fluid model, interfacial concentration is one of the important parameters. The objective of this study is to develop an interfacial area equation with the source and sink terms being properly modeled. For bubble coalescence, the random collisions between bubbles due to turbulence, and the wake entrainment process due to the relative motions of the bubbles, were included. For bubble breakup, the impact of turbulent eddies is considered. Compared with measured axial distributions of the interfacial area concentration under various flow conditions, the adjustable parameters in the source/sink terms were obtained for the simplified one-dimensional transport equation. © 1997 Elsevier Science Ltd.

1. INTRODUCTION

In the analysis of two-phase flow, the formulation using a two-fluid model is considered as the most accurate model. With proper averaging in this model [1–4], the two phases are considered separately in terms of two sets of conservation equations that govern the balance of mass, momentum and energy in each phase. However, the averaged macroscopic fields of the two phases are not independent of each other, and there are certain phase interaction terms in the field equations to characterize the interfacial transfer of mass, momentum and energy. These terms all contain a parameter that specifies the geometric capability of the interfacial transfer, i.e. the interfacial area concentration, defined as the total surface area of the dispersed fluid particles per unit mixture volume [5]. Therefore, a closure relation for the interfacial area concentration is indispensable in the two-fluid model concerning the detailed treatment of the phase interactions.

Since the interfacial area concentration changes with the variation of the particle number density due to coalescence and breakage, analogous to Boltzmann's transport equation, a population balance approach (PBA) was proposed by Reyes [6] to develop a particle number density transport equation for chemically non-reacting, dispersed, spherical fluid particles. A similar method was employed in combustion theory, known as the spray-equation [7]. For the purpose of interfacial area transport, Kocamustafaogullari and Ishii [8] generalized Reyes' model, leading to the following equation:

$$\frac{\partial f(\bar{x}, \mathscr{V}, t)}{\partial t} + \nabla \cdot (f(\bar{x}, \mathscr{V}, t)\mathbf{v}_p) = \sum_j s_j(\bar{x}, \mathscr{V}, t) + s_{ph}(\bar{x}, \mathscr{V}, t) \quad (1)$$

where $f(\bar{x}, \mathscr{V}, t)$ is the particle number density distribution function, which specifies the probable number of fluid particles at a given time t, in the spatial range of $d\bar{x}$ about a position $\bar{x}$, with particle volumes between $\mathscr{V}$ and $\mathscr{V}+d\mathscr{V}$. Moreover, $\mathbf{v}_p(\bar{x}, \mathscr{V}, t)$ denotes the local time-average velocity of the particles, and $s_{ph}(\bar{x}, \mathscr{V}, t)$ refers to the fluid particle sink or source rate due to phase change. If the phase change only causes fluid particle shrinkage or expansion, s_{ph} can be expressed in the form of $-\partial/\partial t(f\, d\mathscr{V}/dt)$, a term Shraiber [9] thought should be presented on the left-hand side of equation (1). However, for the case of homogeneous nucleate boiling or condensation in a subcooled boiling flow, s_{ph} should also include the rate of change of the fluid particle population with specific volumes. Detailed studies on the phase change term follow the approach of Kocamustafaogullari and Ishii [10].

The interaction term, $s_j(\bar{x}, \mathscr{V}, t)$, represents the net rate of change of the particle number density distribution function caused by particle breakup or coalescence process. Some phenomenological models for these terms were summarized by Prince and Blanch [11], and Lafi and Reyes [12]. These models presented

NOMENCLATURE

a	area concentration
C	constant, drag coefficient
D	bubble Sauter mean diameter
f	two-phase friction factor
j	superficial velocity
L	length
n	bubble number density
r	collision frequency for two bubbles
R	collision rate
Re	Reynolds number
s	volume dependent source/sink terms
S	source/sink terms
t	time
T	time
u	velocity
v	velocity
$\mathscr{V}$	bubble volume
We	Weber number
x	space coordinates
z	flow direction coordinate.

Greek symbols

α	void fraction
Δ	difference
ε	averaging factor
μ	dynamic viscosity
ρ	density
σ	surface tension.

Subscripts

a	interfacial area concentration
b	bubble
cr	critical
e	effective
f	liquid
g	gas
h	hydraulic
i	interfacial
m	mixture
max	maximum
n	bubble number density
p	particle/bubble
ph	phase change
pm	bubble mean value
RC	random collision
t	turbulent
TI	turbulent impact
$\mathscr{V}$	bubble volume
w	bubble wake
WE	wake entrainment.

the detailed insight of the mechanisms for coalescence and breakage phenomena. However, due to the dependence on the fluid particle volume, many adjustable parameters and assumptions were imposed that may be beyond justification with the existing experimental data. For most two-phase flow studies, where the primary focus is on the average fluid particle behavior, the detailed volume dependent particle number density transport equation would be too tedious and complicated for use in the field equations. Hence, the present study starts from the following integral form of the particle number density transport equation:

$$\frac{\partial n(\bar{x}, t)}{\partial t} + \nabla \cdot (\mathbf{v}_{\mathrm{pm}}(\bar{x}, t) n(\bar{x}, t)) = \sum_j S_{\mathrm{n},j}(\bar{x}, t) + S_{\mathrm{n,ph}}(\bar{x}, t) \quad (2)$$

where $n(\bar{x}, t)$ is the number density of particles of all sizes, and $\mathbf{v}_{\mathrm{pm}}(\bar{x}, t)$ is the average local particle velocity weighted by the particle number, which is identical to the time-averaged bubble velocity weighted by the gas void fraction, $\bar{\mathbf{v}}_{\mathrm{g}}$, in the time-averaged two-fluid model [3], if the statistical sample size is sufficiently large. On the right-hand side of equation (2), $S_{\mathrm{n},j}$ and $S_{\mathrm{n,ph}}$ represent the total bubble number source or sink rate per unit mixture volume.

To model the integral source and sink terms in equation (2) caused by particle coalescence and breakage, a general approach treats the bubbles in two groups: the spherical/distorted bubble group and the cap/slug bubble group [13], resulting in two bubble number density transport equations that involve the inner and inter group interactions, as shown in Fig. 1. The mechanisms of these interactions can be summarized in five categories: the coalescence due to random collisions driven by turbulence, the coalescence due to wake entrainment, the breakage due to the impact of turbulent eddies, the shearing-off of small bubbles from cap bubbles, and the breakage of large cap bubbles due to flow instability on the bubble surface. Some other mechanisms, such as laminar shearing induced coalescence [14] and the breakage due to velocity gradient [15], are excluded because they are indirectly caused by the distributions of the flow parameters and void fraction [16], and the direct mechanisms still follow the above five categories.

In practice, when the void fraction of a two-phase bubbly flow is small, no cap or slug bubbles exist. The two-group transport equations are then reduced to one group without the involvement of the interactions between the two groups. As the first step of the general approach, the focus of this study is on the first group transport equation for bubbly flow without the occurrence of cap or slug bubbles. In Section two, three models are developed for binary bubble coalescence

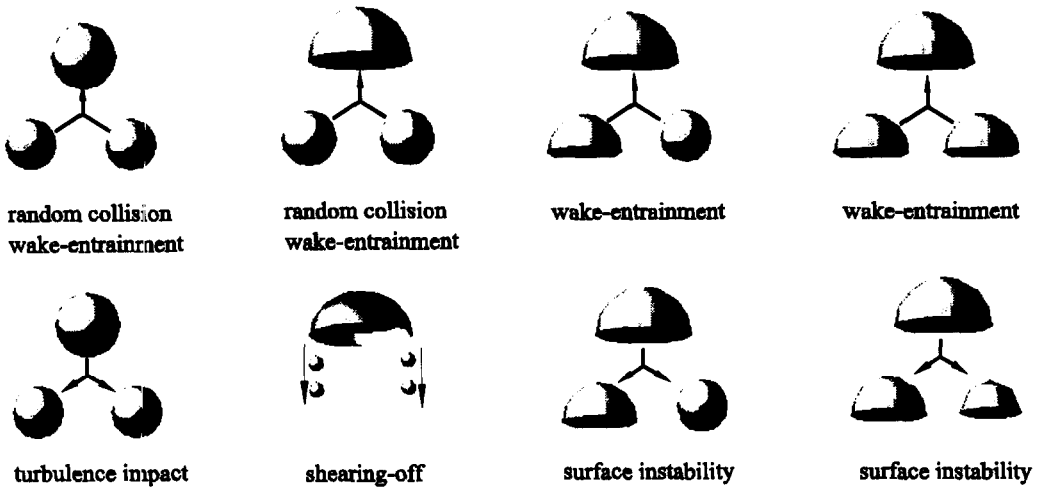

Fig. 1. Mechanisms of bubble coalescence and break-up in two-group model.

and breakage, including the bubble coalescence due to random collisions driven by turbulence, bubble coalescence due to wake entrainment, and bubble breakage due to the impact of turbulent eddies. With these models, the one-group interfacial area transport equation is obtained in Section 3, whereas the adjustable parameters are evaluated in section four with the existing experimental data obtained from vertical two-phase bubbly flow [17]. The approach in this study provides a preliminary foundation for the latter phase investigation of the two-group transport equations, which serve as the general closure relation for interfacial area concentration for the two-fluid model.

2. MODELING OF BUBBLE COALESCENCE AND BREAKAGE

For dispersed bubbly flow without phase change, only three mechanisms for bubble coalescence and breakage are considered in the following one-group bubble number density transport equation:

$$\frac{\partial n(\bar{x},t)}{\partial t}+\nabla\cdot(\bar{v}_g(\bar{x},t)n(\bar{x},t)) = S_{n,RC}(\bar{x},t)+S_{n,WE}(\bar{x},t)+S_{n,TI}(\bar{x},t) \quad (3)$$

where the subscript 'n' stands for net bubble number density change, 'RC' for random collision due to turbulence in the continuous medium, 'WE' for wake-entrainment, and 'TI' for turbulent eddies that impact on bubbles resulting in bubble breakage. In this section, these source and sink terms are modeled individually by assuming binary spherical bubble interactions. Throughout the study, the average bubble size is characterized by the bubble Sauter mean diameter, $D \equiv 6\alpha/a_i$, where α and a_i represent the local time-averaged void fraction and interfacial area concentration, respectively.

2.1. *Random collision induced bubble coalescence*

To model the bubble coalescence rate induced by turbulence in the continuous medium, the bubble random collision rate is of primary importance. These collisions are postulated to occur only between the neighbouring bubbles, because long range interactions are driven by large eddies that transport groups of bubbles without leading to significant relative motion [11, 18]. Between two neighboring spherical bubbles of the same size as shown in Fig. 2, the time interval for one collision, Δt, is defined as

$$\Delta t = \bar{L}/u_t. \quad (4)$$

Here, u_t is the root-mean-square approaching velocity of the two bubbles, and $\bar{L}$ represents the mean travelling distance between the two bubbles for one collision, which is approximated by:

$$\bar{L} \approx De-\delta D \propto \left(\frac{D}{\alpha^{1/3}}-\delta_1 D\right)=\frac{D}{\alpha^{1/3}}(1-\delta_1\alpha^{1/3}) \quad (5)$$

where De denotes the effective diameter of the mixture volume that contains one bubble. Since the bubble travelling length for one collision varies from De to

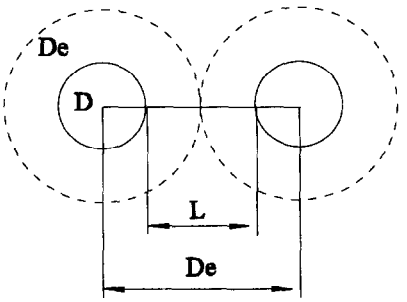

Fig. 2. Geometric definitions of two approaching bubbles.

$(De-D)$, a factor δ is introduced in equation (5) to feature the average effect, whereas δ_1 is a collective parameter in considering the sign of proportionality between De and $D/\alpha^{1/3}$. For small void fraction, δ_1 plays a minor role due to the fact that De is much larger than D. However, it is important if the travelling length is comparable to the mean bubble size. When void fraction approaches the dense packing limit ($\alpha \cong \alpha_{max}$), the mean travelling length should be zero, which leads to δ_1 equal to $\alpha_{max}^{-1/3}$. Using this asymptotic value as the approximation of δ_1, the mean travelling length is reduced to:

$$\bar{L} \propto \frac{D}{\alpha^{1/3}}\left[1-\left(\frac{\alpha}{\alpha_{max}}\right)^{1/3}\right]. \tag{6}$$

Accordingly, the collision frequency for two bubbles moving toward each other is given by:

$$r_{RC} = \frac{1}{\Delta t} \propto \frac{u_t}{D}\alpha^{1/3}\left[\frac{\alpha_{max}^{1/3}}{\alpha_{max}^{1/3}-\alpha^{1/3}}\right]. \tag{7}$$

Since the bubbles do not always move toward each other, however, a probability, P_c, for a bubble to move toward a neighboring bubble is considered here to modify the collision rate. By assuming a hexagonal close-packed structure, this probability is given by:

$$P_c \sim \frac{D^2}{De^2} = \alpha^{2/3}, \alpha < \alpha_c, \quad \text{and} \quad P_c = 1, \alpha > \alpha_c \tag{8}$$

where α_c is the critical void fraction when the center bubble cannot pass through the free space among the neighboring bubbles. In reality, the neighboring bubbles are in constant motion, and the critical void fraction can be very close to the dense packing limit. This leads to:

$$P_c \propto \left(\frac{\alpha}{\alpha_{max}}\right)^{2/3}. \tag{9}$$

Subsequently, the collision rate for a mixture with bubble number density, n, is given by:

$$R_{RC} \approx \frac{u_t}{\bar{L}} n P_c \propto n u_t \frac{\alpha}{D}\left[\frac{1}{\alpha_{max}^{1/3}(\alpha_{max}^{1/3}-\alpha^{1/3})}\right]$$

$$\propto n^2 u_t D^2\left[\frac{1}{\alpha_{max}^{1/3}(\alpha_{max}^{1/3}-\alpha^{1/3})}\right]. \tag{10}$$

The functional dependence of the above collision rate agrees with that of Coulaloglou and Tavlarides [18] proposed in 1976 for a liquid–liquid droplet flow system, analogous to the particle collision model in an ideal gas. The difference is that the present model contains an extra term in the bracket, which covers the situation when the mean free path of a bubble is comparable to the mean bubble size. Nevertheless, the model in the present form is still incomplete, since no matter how far away the neighboring bubble is located, the collision would occur as long as there is a finite approaching velocity. In actuality, when the mean distance is very large, no collision should be counted because the range of the relative motion for collisions between the neighboring bubbles is limited by the eddy size comparable to the bubble size. To consider this effect, the following modification factor is suggested for equation (10):

$$\left[1-\exp\left(-C\frac{L_t}{\bar{L}}\right)\right] \tag{11}$$

where L_t is the average size of the eddies that drive the neighboring bubbles together, which is assumed to be on the same order of the mean bubble size, because smaller eddies do not provide considerable bulk motion to a bubble, while larger eddies transport groups of bubbles without significant relative motion. Thereafter, the final form of the bubble collision rate is given by:

$$R_{RC} \sim (u_t n^2 D^2)\left[\frac{1}{\alpha_{max}^{1/3}(\alpha_{max}^{1/3}-\alpha^{1/3})}\right]$$

$$\times\left[1-\exp\left(-C\frac{\alpha_{max}^{1/3}\alpha^{1/3}}{\alpha_{max}^{1/3}-\alpha^{1/3}}\right)\right]. \tag{12}$$

For each collision, coalescence may not occur and thus a collision efficiency was suggested by many investigators [19, 20]. The most popular model for the collision efficiency is the film thinning model [20]. In this model when the bubbles approach faster, they tend to bounce back without coalescence due to the limitation of the film drainage rate governed by the surface tension. Mathematically, the coalescence rate decreases exponentially with respect to the turbulent fluctuating velocity, which is much stronger than the linear dependence of the collision rate, resulting in an overall decreasing trend of the coalescence rate as the turbulent fluctuation increases. This caused serious trouble when the model was applied to experimental data following the procedure specified in Section 4. Tremendous discrepancies were obtained at different liquid flow conditions. Hence, a constant coalescence efficiency is employed in the present model to depict the randomness of the coalescence phenomenon after each collision [16], and the bubble coalescence rate due to random collisions is given by:

$$R_{RC} = C_{RC}(u_t n^2 D^2)\left[\frac{1}{\alpha_{max}^{1/3}(\alpha_{max}^{1/3}-\alpha^{1/3})}\right]$$

$$\times\left[1-\exp\left(-C\frac{\alpha_{max}^{1/3}\alpha^{1/3}}{\alpha_{max}^{1/3}-\alpha^{1/3}}\right)\right] \tag{13}$$

where C_{RC} and C are adjustable parameters, depending on the properties of the fluid. Nevertheless, the constant coalescence efficiency is only an approximation, and further efforts are needed to model the efficiency mechanistically. The remaining unknowns are the maximum void fraction and the mean bubble fluctuating velocity. By definition, α_{max} is the dense packing limit of void fraction when the coalescence

rate approaches infinity. A rational choice of α_{max} should be approximately 0.8 at the transition point from slug to annular flow [16, 21]. The mean bubble fluctuating velocity, u_t, in equation (13), is proportional to the root-mean-square liquid fluctuating velocity difference between two points of length scale D, and is given by $\varepsilon^{1/3}D^{1/3}$ [13]. Here, ε is the energy dissipation rate per unit mass of the continuous medium. In a complete two-fluid model, ε comes from its own constitutive relation such as the two-phase κ–ε model [22, 23]. For one-dimensional analysis, however, this term can be approximated by a simple algebraic equation, as suggested in Section 4.

2.2. *Wake-entrainment induced bubble coalescence*

When bubbles enter the wake region of a leading bubble, they will accelerate and may collide with the preceding one [24–26]. For a spherical air bubble with attached wake region in the liquid medium, the effective wake volume, $\mathscr{V}_w$, in which the following bubbles may collide with the leading one, is defined as the projected bubble area multiplied by the effective length, L_w. The number of bubbles inside the effective volume is then given by

$$N_w = \mathscr{V}_w n \approx \frac{1}{4}\pi D^2 (L_w - D/2) n. \tag{14}$$

Assuming that the average time interval for a bubble in the wake region to catch up with the preceding bubble is ΔT, the collision rate per unit mixture volume should satisfy:

$$R_{WE} \propto \frac{1}{2} n \frac{N_w}{\Delta T} \approx \frac{1}{8}\pi D^2 n^2 \left(\frac{L_w - D/2}{\Delta T}\right) \approx \frac{1}{8}\pi D^2 n^2 \bar{u}_{rw} \tag{15}$$

where $\bar{u}_{rw}$ is the average relative velocity between the leading bubble and the bubble in the wake region. If the transient for a bubble to reach its terminal velocity is assumed to be much shorter than the collision process, the average relative velocity, $\bar{u}_{rw}$, can be expressed in terms of the relative velocities of the continuous medium inside and outside the wake region:

$$\bar{u}_{rw} \approx \overline{(V_f(z) - V_{f0})} \tag{16}$$

with $V_f(z)$ as the local liquid velocity along the center line, z as the distance measured from the center of the leading bubble, and V_{f0} as the ambient liquid velocity. For spherical bubbles, since the external flow is almost indistinguishable from that around a solid sphere at the same Reynolds number [27], the wake structure of the leading bubble can be analogous to that around a solid sphere. In such a turbulent wake ($Re_D > 20$), which satisfies most of the practical bubbly flow regimes, the wake velocity along the center line roughly satisfies [28]:

$$V_f(z) - V_{f0} = u_r(D)\left(\frac{D/2}{z}\right)^{2/3}. \tag{17}$$

Here, $u_r(D)$ is the terminal velocity of a bubble of diameter D relative to the liquid motion. By integrating equation (17) over the effective wake length, the average relative velocity in the wake region is given by:

$$\bar{u}_{rw} \approx u_r(D)\left(\frac{3D/2}{L_w - D/2}\right)\left[\left(\frac{L_w}{D/2}\right)^{1/3} - 1\right] = u_r(D) F\left(\frac{D}{L_w}\right). \tag{18}$$

The exact form of $F(D/L_w)$ is not important since the effective bubble wake region may not be fully established. According to Tsuchiya [29], the wake length is roughly 5–7 times the bubble diameter in an air–water system, and thus D/L_w as well as $F(D/L_w)$ are treated as constants depending on the fluid properties. As long as their values obtained from experimental data fall into the range of $D/L_w = 5$–7, the mechanism should be acceptable. Substituting equation (18) into equation (15) yields the following simple expression of the bubble collision rate per unit mixture volume due to the wake-entrainment mechanism:

$$R_{WE} = C_{WE} D^2 u_r(D) n^2, \quad \text{with } C_{we} = \frac{1}{8} F\left(\frac{D}{L_w}\right) \tag{19}$$

where C_{WE} is an adjustable constant mainly determined by the ratio of the effective wake length to the bubble size and the coalescence efficiency. A proper choice for C_{WE} should yield an effective wake length roughly between 5 and 7 from equations (19) and (18). The bubble terminal velocity, u_r, is a function of the bubble diameter and local time-average void fraction. Based on the balance between the buoyancy force and drag force in a two-phase bubbly flow, Ishii and Chawla [30] applied a drag-similarity criterion with the mixture-viscosity concept to obtain the following expression for the relative velocity:

$$u_r = \left(\frac{Dg}{3C_D}\frac{\Delta\rho}{\rho_f}\right)^{1/2} \tag{20}$$

$$C_D = 24\frac{(1 + 0.1 Re_D^{0.75})}{Re_D} \quad \text{and} \quad Re_D \equiv \frac{\rho_f u_r D}{\mu_f}(1-\alpha). \tag{21}$$

2.3. *Bubble breakup due to turbulent impact*

For binary bubble breakup due to the impact of turbulent eddies, the driving force comes from the inertial force, F_t, of the turbulent eddies in the continuous medium, while the holding force is the surface tension force, F_σ. To drive the daughter bubbles apart with a characteristic length of D within time interval Δt, a simple momentum balance approach gives the following relation:

$$\frac{\rho_f D^3 D}{\Delta T^2} \propto F_t - F_\sigma. \tag{22}$$

Here, the inertia of the bubble is dominated by the virtual mass because of the large density ratio of the liquid and gas. Rearranging equation (22) leads to the following average bubble breakup time:

$$\Delta T \propto \frac{D}{u_t}\left(1-\frac{We_{cr}}{We}\right)^{-1/2}, \quad We=\frac{\rho_f u_t^2 D}{\sigma} > We_{cr}. \tag{23}$$

The velocity, u_t is assumed to be the root-mean-square velocity difference between two points of length D, which implies that only the eddies with sizes equivalent to the bubble size can break the bubble. We_{cr} is a collective constant, designated as a critical Weber number. The reported value of We_{cr} for bubble breakup varies in a wide range due to the resonance excitation of the turbulent fluctuation [31]. In an air–water system, Prince and Blanch [11] suggested that We_{cr} equals 2.3. Accordingly, if the bubble number density is n, the bubble breakup rate should be:

$$R_{TI} \propto n\frac{1}{\Delta T} = n\frac{u_t}{D}\left(1-\frac{We_{cr}}{We}\right)^{1/2}, \quad We > We_{cr}. \tag{24}$$

In a homogeneous turbulent flow, the probability for a bubble to collide with an eddy that has sufficient energy to break the bubble is approximately [18]:

$$\eta_{ti} \propto \exp\left(-\frac{u_{t,cr}^2}{u_t^2}\right) \tag{25}$$

where $u_{t,cr}^2$ is the critical mean-square fluctuation velocity obtained from We_{cr}. Finally, the bubble breakup rate per unit mixture volume is given by:

$$R_{TI} = C_{TI}\exp\left(-\frac{We_{cr}}{We}\right)n\frac{u_t}{D}\left(1-\frac{We_{cr}}{We}\right)^{1/2}, \quad We > We_{cr}. \tag{26}$$

Again, the adjustable parameters C_{TI} and We_{cr} should be evaluated with experimental data. This expression differs from the previous models [11, 12] because the breakup rate equals zero when the Weber number is less than We_{cr}. This unique feature permits the decoupling of the bubble coalescence and breakup processes. At a low liquid flow rate with small void fraction, the turbulent fluctuation is small and thus no breakup would be counted, which allows the fine-tuning of the adjustable parameters in the coalescence terms, independent of the bubble breakage.

3. ONE-GROUP INTERFACIAL AREA CONCENTRATION TRANSPORT EQUATION

In the two-fluid model, the parameter of interest is the interfacial area, a_i, rather than the bubble number density. To obtain the transport equation for interfacial area concentration, equation (2) can be modified with the following geometric relation:

$$n = \frac{\alpha}{\mathscr{V}_b} = \psi\left(\frac{a_i^3}{\alpha^2}\right) \tag{27}$$

where ψ is a factor depending on the shape of the bubbles, and $\mathscr{V}_b$ denotes the average bubble volume. For spherical bubbles ψ equals $1/(36\pi)$. Substituting equation (27) into equation (2) yields:

$$\frac{\partial a_i}{\partial t}+\nabla\cdot(a_i\bar{\mathbf{v}}_g) = \frac{1}{3\psi}\left(\frac{\alpha}{a_i}\right)^2\left[\sum_j S_{n,j}+S_{n,ph}\right] + \left(\frac{2a}{3\alpha}\right)\left[\frac{\partial\alpha}{\partial t}+\nabla\cdot(\bar{\mathbf{v}}_g\alpha)\right]. \tag{28}$$

The second term on the right-hand side represents the effects of the variation in bubble volume. If the gas phase is assumed to be incompressible without phase change, from the gas phase continuity equation, this term should be zero. Subsequently, the one-group interfacial area transport equation is reduced to:

$$\frac{\partial a_i}{\partial t}+\nabla\cdot(a_i\bar{\mathbf{v}}_g) = \frac{1}{3\psi}\left(\frac{\alpha}{a_i}\right)^2(-R_{RC}-R_{WE}+R_{TI}) = S_{a,RC}+S_{a,WE}+S_{a,TI}. \tag{29}$$

With the models developed in Section 2, the net rates of change of interfacial area concentration per unit mixture volume are given below:

$$S_{a,RC} = -\frac{1}{3\pi}C_{RC}(u_t a_i^2)\left[\frac{1}{\alpha_{max}^{1/3}(\alpha_{max}^{1/3}-\alpha^{1/3})}\right]\times\left[1-\exp\left(-C\frac{\alpha_{max}^{1/3}\alpha^{1/3}}{\alpha_{max}^{1/3}-\alpha^{1/3}}\right)\right]. \tag{30}$$

$$S_{a,WE} = -\frac{1}{3\pi}C_{WE}u_r a_i^2. \tag{31}$$

$$S_{a,TI} = \frac{1}{18}C_{TI}u_t\left(\frac{a_i^2}{\alpha}\right)\left(1-\frac{We_{cr}}{We}\right)^{1/2}\times\exp\left(-\frac{We_{cr}}{We}\right), \quad We > We_{cr}. \tag{32}$$

Equations (29)–(32) constitute the one-group closure relation of interfacial area concentration in two-phase vertical dispersed bubbly flow. The variables in these equations are coupled with the field equations in the two-fluid model. For the information of the local interfacial area concentration, the field equations should be solved together with the closure relations. However, the presented model is limited to the two-phase dispersed bubbly flow. At high void fraction when cap or slug bubbles appear, another transport equation should be provided for the interfacial area concentration of cap or slug bubbles. The two groups are not independent and the inter-group transfer terms should also be modeled individually.

4. EVALUATION OF THE ONE-GROUP MODEL

The simplest form of the interfacial area transport equation is the one-dimensional formulation obtained by applying cross-sectional area averaging over equation (29):

$$\frac{\partial\langle a_i\rangle}{\partial t}+\frac{\partial}{\partial z}(\langle a_i\rangle\langle\langle v_{gz}\rangle\rangle_a) = \langle S_{a,RC}\rangle+\langle S_{a,WE}\rangle+\langle S_{a,TI}\rangle. \quad (33)$$

Due to the uniform bubble size assumption, the area-averaged bubble interface velocity weighted by interfacial area concentration can be given by:

$$\langle\langle v_{gz}\rangle\rangle_a \equiv \frac{\langle a_i v_{gz}\rangle}{\langle a_i\rangle} \approx \frac{\langle\alpha v_{gz}\rangle}{\langle\alpha\rangle}\langle\langle v_g\rangle\rangle \quad (34)$$

which is the same as the conventional area-averaged gas velocity weighted by void fraction, if the internal circulation in the bubble is neglected. The exact mathematical expressions for the area-averaged source and sink terms would involve many covariances that may further complicate the one-dimensional problem. However, since these local terms were originally obtained from a finite volume element of the mixture, the functional dependence of the area-averaged source and sink terms on the averaged parameters should be approximately the same if the hydraulic diameter of the flow path is considered as the length scale of the finite element. Therefore, equations (30)–(32) with the parameters averaged within the cross-sectional area are still applicable for the area-averaged source and sink terms in equation (33).

To utilize the experimental data at different axial locations under steady-state condition, the transient term in equation (33) has to be dropped, resulting in

$$\frac{\mathrm{d}}{\mathrm{d}z}(\langle a_i\rangle\langle\langle v_{gz}\rangle\rangle) = \langle S_{a,RC}\rangle+\langle S_{a,WE}\rangle+\langle S_{a,TI}\rangle. \quad (35)$$

Without phase change, under the assumption of incompressible flow, the void fraction should be constant, independent of the axial positions. For a given flow condition, the only variable that should be specified is the energy dissipation rate per unit mixture mass, ε. A sophisticated approach is to couple the transport equation with the field equations and the constitutive relation of ε, such as k–ε model [25]. However, for the purpose of evaluating the model in the one-dimensional form, a simple algebraic correlation for ε is employed in this study:

$$\varepsilon = f_{TW}\frac{1}{2D_h}\langle v_m\rangle^3 \quad (36)$$

where $\langle v_m\rangle$ is the mean mixture velocity, D_h refers to the hydraulic diameter of the flow path, and f_{TW} is the two-phase friction factor. With μ_m as the mixture viscosity [30], f_{TW} is given by:

$$f_{TW} = f_f\left(\frac{\mu_m}{\mu_f}\right)^{0.25} = \frac{0.316}{Re_m^{0.25}}\left(\frac{1}{(1-\langle\alpha\rangle}\right)^{0.25}. \quad (37)$$

To identify the adjustable parameters in the source and sink terms, experimental data of a steady air–water cocurrent up-flow in a 5.08 cm pipe [17] are used. In these experiments, interfacial area concentration and void fraction were measured with a double-sensor conductivity probe at three different axial positions ($L/D_h = 2$, 32, 62). In Table 1, seven cases of tests are summarized for different flow conditions. With the measured interfacial area concentration at $L/D_h = 2$ as the initial condition, equation (35) is integrated numerically to predict the axial distribution of interfacial area concentration, and the adjustable parameters are determined if the predictions at the other two locations match the experimental data. At low liquid flow rate with small void fraction, bubble breakage can be neglected due to the very small Weber number compared to the critical value. Therefore, the fitting involves only three constants: C_{RC}, C and C_{WE}. After these parameters are fixed, the transport equation is further applied to high flow rate conditions solely for C_{TI} and We_{cr}. The final results of these adjustable parameters are summarized in Table 1. For the wake-entrainment mechanism, C_{WE} is 0.151. Assuming a flat cross-sectional wake velocity profile, the effective wake length for bubble coalescence as estimated from equations (18) and (19) is about seven times the bubble diameter, which agrees with the observation of Tsuchiya [29]. For bubble breakup, the critical Weber number is found to be 2.0 for the best fitting to the experimental data, which is slightly smaller than 2.3, a value suggested by Prince and Blanch [11]. This discrepancy may be caused by the one-group approach that assumes uniform bubble size. In reality, bubble breakage exists as long as the size of certain bubbles reaches the breakup limit in spite of the fact that the mean size does not exceed it. Therefore, the critical Weber number for bubble breakage based on the average bubble size should be smaller than that from the actual size of a breaking bubble.

At a very low liquid flow rate with small void fraction, as in the case 1, no bubble breakage is involved.

Table 1. Test conditions [17] and adjustable parameters

	$\langle j_g\rangle$ (m s^{-1})	$\langle j_f\rangle$ (m s^{-1})	$\langle\alpha\rangle$
Case 1	0.023	0.77	2.5%
Case 2	0.117	0.77	10.0%
Case 3	0.058	1.11	4.0%
Case 4	0.117	1.11	7.0%
Case 5	0.023	1.58	1.6%
Case 6	0.058	1.58	3.0%
Case 7	0.117	1.58	6.5%

C_{RC}	C	C_{WE}	We_{cr}	C_{TI}
0.0565	3	0.151	0.18	2.0

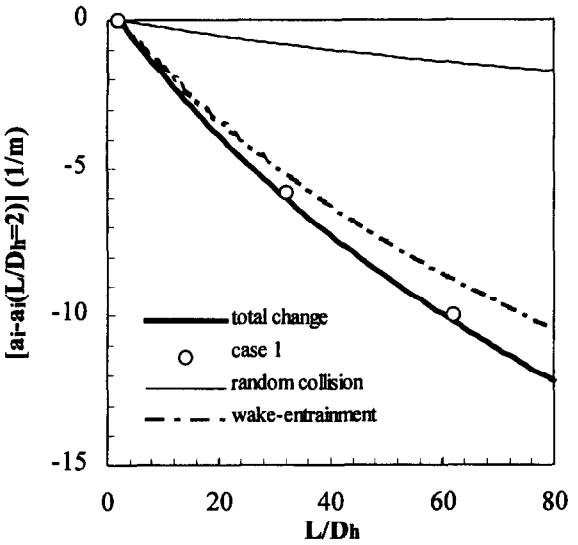

Fig. 3. Axial variation of $\langle a_i \rangle$ for case 1.

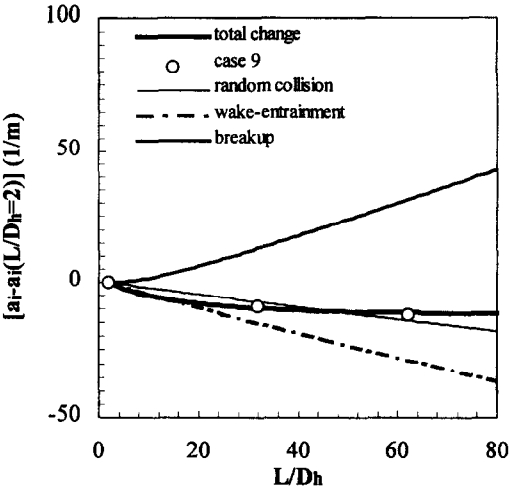

Fig. 5. Axial variation of $\langle a_i \rangle$ for case 7.

Figure 3 illustrates such variation of the area-averaged interfacial area concentration in the flow direction. With the selected coefficients, no bubble breakage is present since the Weber number is smaller than the critical value. Since the void fraction is small, the change of interfacial area concentration caused by random collisions is only about one tenth of total decrease. However, as the void fraction increases to 10% in case 2 with the same liquid superficial velocity as in case 1, the change of interfacial area concentration due to random collisions increases to roughly 20% of the total change, as shown in Fig. 4. Moreover, because of the large coalescence rate, the mean bubble size grows rapidly. At about $L/D_h = 40$, the bubble Weber number becomes greater than the critical value and thus the bubble breakage term must be taken into account, resulting in a slower decrease of the interfacial area concentration in the flow direction. An extreme condition is for case 7, as shown in Fig. 5, with a liquid superficial velocity of 1.58 m s^{-1}, where bubble breakage exists at the very beginning. In this case, the coalescence rate seems balance by the breakup rate along the flow path, resulting in a relatively flat axial distribution of the interfacial area concentration. Compared to the experimental data, all seven cases are shown in Figs. 6(a) and (b). The interfacial area concentrations predicted by the proposed model are generally in good agreement with the measurements at three axial positions. The maximum relative difference is about 8% at very small void fraction with high liquid flow rate. Nevertheless, the conclusion is based on the only set of published experimental data that have three axial measurements for each flow condition. Fine-tuning of the adjustable parameters is needed as more data become available. Moreover, the constant coalescence efficiency is only an approximation, and further efforts are needed to model the efficiency mechanistically.

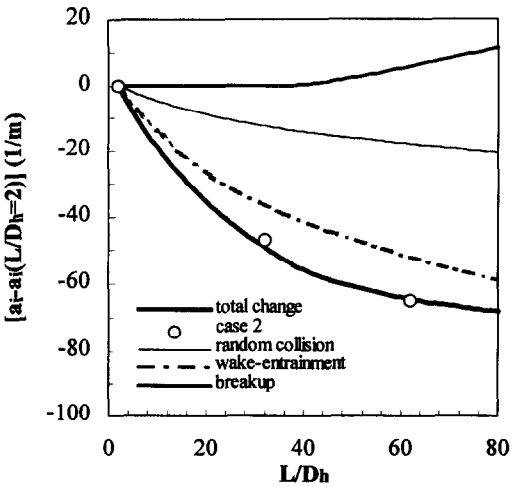

Fig. 4. Axial variation of $\langle a_i \rangle$ for case 2.

5. CONCLUSIONS

In this study, a one-group interfacial area transport equation together with the modeling of the source and sink terms for bubble breakup and coalescence was presented. For bubble coalescence, two mechanisms were considered to be dominant in the vertical two-phase bubbly flow: the random collisions between bubbles due to turbulence in the flow field and the wake entrainment process due to the relative motion of the bubbles in the wake region of a seeding bubble. For bubble breakup, the impact of turbulent eddies was included.

By area-averaging over the local one-group transport equation, a one-dimensional form of the interfacial area concentration transport equation was obtained. Compared with experimental data for the

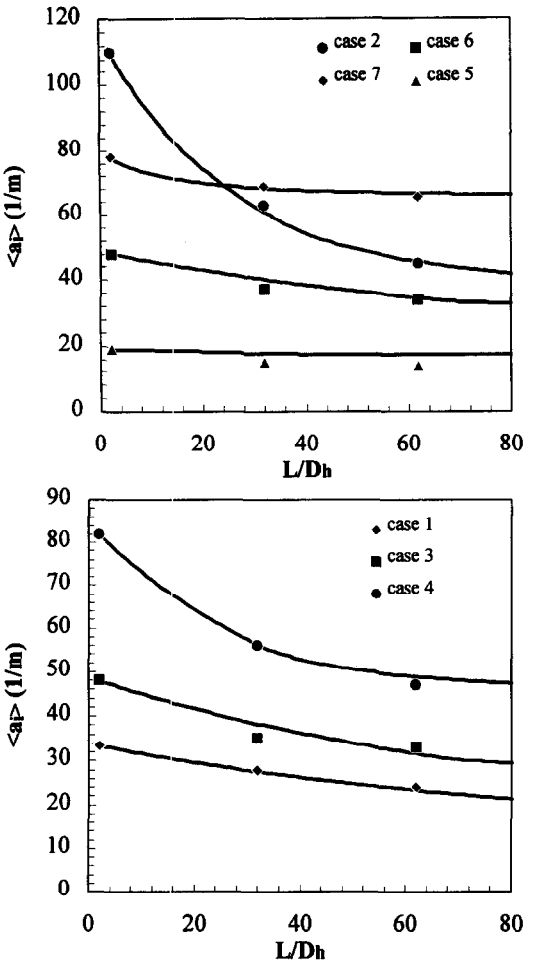

Fig. 6. (a) Axial variation of $\langle a_i \rangle$ for case 2, 5, 6 and 7; (b) axial variation of $\langle a_i \rangle$ for case 1, 3 and 4.

axial distribution of the interfacial area concentration under various flow conditions, the adjustable parameters in the model were obtained. The results indicate that the proposed models for bubble breakup and coalescence are appropriate. The ranges of the adjustable parameters agree with the physical observations. However, the comparison was based on the only set of published experimental data that have three axial measurements for each flow condition. Fine-tuning of these adjustable parameters is needed as more data becomes available. When applied to three-dimensional cases, the adjustable parameters for the detailed localized transport equation have to be verified through the coupling with the two-fluid model. Moreover, the constant coalescence efficiency in this study is only an approximation, and further efforts are needed to model the efficiency mechanistically.

Acknowledgements—This study was supported by Westinghouse Bettis Atomic Power Laboratory. Valuable comments of Ms T. Wilmarth de Leonardi are appreciated.

REFERENCES

1. Vernier, P. and Delhaye, J. M., General two-phase flow equations applied to the thermohydrodynamics of boiling nuclear reactor. *Energie Primaire*, 1968, **4**, 5–25.
2. Kocamustafaogullari, G., Thermofluid dynamics of separated two-phase flow. Ph.D thesis, Georgia Institute of Technology, Atlanta, GA, 1971.
3. Ishii, M., *Thermo-Fluid Dynamic Theory of Two-Phase Flow*. Collection de la Direction des Etudes et Reserches d'Electricité de France, Eyrolles, Paris, 22, 1975, p.45.
4. Boure, J. A., Mathematical modeling of two-phase flows. *Proceedings of CSNI Specialist Meeting*, ed. S. Banerjee and K. R. Weaver, Vol. 1. A.E.C.L., Toronto, Canada, 1978, p. 85.
5. Ishii, M. and Mishima, K., Study of two-fluid model and interfacial area. Technical report. ANL-80-111, Argonne National Laboratory, Chicago, IL, 1980.
6. Reyes, J. N., Statistically derived conservation equations for fluid particle flows. *Proceedings of ANS Winter Meeting*, San Francisco, CA, 1989, p. 12.
7. Williams, F. A., *Combustion Theory*, Addison-Wesley, Reading, MA, 1965.
8. Kocamustafaogullari, G. and Ishii, M., Foundation of the interfacial area transport equation and its closure relation. *International Journal of Heat and Mass Transfer*, 1995, **38**, 481.
9. Shraiber, A. A., Comments on 'foundation of the interfacial area transport equation and its closure relations'. *International Journal of Heat and Mass Transfer*, 1996, **39**, 1117.
10. Kocamustafaogullari, G. and Ishii, M., Interfacial area and nucleation site density in boiling systems. *International Journal of Heat and Mass Transfer*, 1983, **26**, 1377.
11. Prince, M. J. and Blanch, H. W., Bubble coalescence and break-up in air-sparged bubble columns. *AIChE Journal*, 1990, **36**, 1485.
12. Lafi, A. Y. and Reyes, Jr, J. N., Phenomenological models for fluid particle coalescence and breakage. Technical report, OSU-NE-9120, Department of Nuclear Engineering, Oregon State University, Corvallis, Oregon, 1991.
13. Ishii, M. and Kojasoy, G., Interfacial area transport equation and preliminary considerations for closure relations. Technical report, PU-NE-93/6, Nuclear Engineering Department, Purdue University, West Lafayette, IN, 1993.
14. Friedlander, S. K., *Smoke, Dust and Haze*. Wiley, New York, 1977.
15. Taylor, G. I., The formation of emulsion in definable field of flow. *Proceedings of Royal Society, (London) Series*, 1934, **A146**, 501.
16. Wu, Q., Kim, S., Ishii, M. and Beus, S. G., One-group interfacial area concentration transport in vertical air-water bubbly flow. International Heat Transfer Conference, HTC-Vol. 10, Baltimore, Maryland, 1997, p. 67.
17. Kashyap, A., Ishii, M. and Revankar, S. T., An experimental and numerical analysis of structural development of two-phase flow in a pipe. Technical report, PU-NE-94/2, Nuclear Engineering Department, Purdue University, West Lafayette, IN, 1994.
18. Coulaloglu, C. A. and Tavlarrides, L. L., Drop size distributions and coalescence frequencies of liquid–liquid dispersion in flow vessels. *AIChE Journal*, 1976, **22**, 289.
19. Oolman, T. and Blanch, H. W., Bubble coalescence in stagnant liquids. *Chemical Engineering Communication*, 1986, **43**, 237.
20. Kirkpatrick, R. D. and Lockett, M. J., The influence of approach velocity on bubble coalescence. *Chemical Engineering Science*, 1974, **29**, 2363.
21. Wallis, G. B., *One-dimensional Two-phase Flow*. McGraw-Hill, New York, 1969.

22. Serizawa, A. and Kataoka, I., Turbulence suppression in bubbly two-phase flow. *Journal of Nuclear Engineering and Design*, 1991, **122,** 1.
23. Lopez de Bertodano, M., Lahey, Jr, R. T. and Jones, O. C., Development of a k–ε model for bubbly two-phase flow. *Journal of Fluids Engineering*, 1994, **116,** 128.
24. Otake, T., Tone, S., Nakao, K. and Mitsuhashi, Y., Coalescence and breakup of bubbles in liquids. *Chemical Engineering Science*, 1977, **32,** 377.
25. Bilicki, Z. and Kestin, J., Transition criteria for two-phase flow patterns in vertical upward flow. *International Journal of Multiphase Flow*, 1987, **13**(3), 283.
26. Stewart, C. W., Bubble interaction in low-viscosity liquid. *International Journal of Multiphase Flow*, 1995, **21,** 1037.
27. Clift, R., Grace, J. R. and Weber, M. E., *Bubbles, Drops and Particles.* Academic Press, New York, 1978.
28. White, F. M., *Viscous Fluid Flow*, 2nd edn. McGraw-Hill, New York, 1991, p. 481.
29. Tsuchiya, K., Miyahara, T. and Fan, L. S., Visualization of bubble-wake interactions for a stream of bubble in a two-dimensional liquid solid fluidized bed. *International Journal of Multiphase Flow*, 1989, **15,** 35.
30. Ishii, M. and Chawla, T. C., Local drag laws in dispersed two-phase flow. Technical report, ANL-79-105, Argonne National Laboratory, Chicago, 1979.
31. Sevik, M. and Park, S. H., The splitting of drops and bubbles by turbulent fluid flow. *Journal of Fluids Engineering*, 1973, **95,** 53.